Metabolic cost calculations of gait using musculoskeletal energy models, a comparison study

Anne D. Koelewijn[1,2], Dieter Heinrich [3], Antonie J. van den Bogert[*1]

1 Parker Hannifin Laboratory for Human Motion and Control, Department of Mechanical Engineering, Cleveland State University, Cleveland, Ohio, USA

2 Biorobotics Laboratory, Institute of Bioengineering, École Polytechnique Fédérale de Lausanne, Lausanne, Switzerland

3 Department of Sport Science, University of Innsbruck, Innsbruck, Austria

¤Current Address: 2121 Euclid Ave. FH 243, Cleveland, OH 44115, USA

* a.vandenbogert@csuohio.edu

Abstract

This paper compares predictions of metabolic energy expenditure in gait using seven metabolic energy expenditure models to assess their correlation with experimental data. Ground reaction forces, marker data, and pulmonary gas exchange data were recorded for six walking trials at combinations of two speeds, 0.8 m/s and 1.3 m/s, and three inclines, -8% (downhill), level, and 8% (uphill). The metabolic cost, calculated with the metabolic energy models was compared to the metabolic cost from the pulmonary gas exchange rates. A repeated measures correlation showed that the model by Bhargava et al. [7] and the model by Lichtwark and Wilson [21] correlated best with the experimental data. It was found that for all metabolic energy models, the subject's weight affected the calculated metabolic cost.

Introduction

Humans prefer to walk in energetically optimal ways. Walking speed [1], the ratio between step length and frequency [2], step width [3] and vertical movement of the

center of mass [4, 5] are chosen to minimize energy expenditure. Whole-body energy expenditure can be measured using direct calorimetry, by measuring the heat production in the body, or indirect calorimetry, by measuring the volume of oxygen inspired and carbon dioxide expired [6]. However, these measurements are not always available, but an accurate prediction of energy expenditure is often desired.

Instead, musculoskeletal modeling can be used to simulate human gait and to calculate the energy expenditure based on a metabolic energy expenditure model (e.g., [7–10]). These calculations are based on variables that are studied in gait analysis, such as joint moments, joint power, or muscle forces, lengths and activations [11]. With a metabolic energy expenditure model, the energy expenditure can be calculated for gait experiments that did not take metabolic energy expenditure measurements, or for predictive gait simulations, where no experimental data is available. Recently, these simulations have been used to analyze 'what-if scenarios' such as the effect of an intervention such as a prosthesis [12], an exoskeleton [13], ankle foot orthosis [14], additional weight [15], loaded and inclined walking [16], or changing the gait pattern to minimize knee reaction force [17] on gait. Energy cost is an important variable in gait, and should be considered whenever a clinical intervention is studied or designed.

In literature several energy models were suggested. The Huxley crossbridge model [18] finds both the muscle force and the energy expenditure of a muscle, but requires up to 18 states [19]. Instead, Hill-type muscle models [20] are typically used to simulate muscles, but these do not output metabolic energy expenditure. Therefore, several metabolic energy expenditure models have been proposed that calculate the energy expenditure during walking based on Hill-type muscles [7–10, 21, 22], based on muscle efficiency [23], or based on joint angles and moments [24]. An additional model is based on another, similar muscle model [25]. An additional advantage of metabolic energy expenditure models is their ability to calculate the energy expenditure of single muscles [22], or joints [26] and provide more information than measurements of pulmonary gas exchange, which only calculated on the whole body energy expenditure.

So far, these models have only been compared and used on level walking studies and self-selected speed (e.g. [7, 9, 26]). However, it is important to know how well these models can represent changes in energy cost due to altered control, such as a change in walking speed, or environment. If this is done accurately, these models can be used to

assess the energetic effect of an intervention.

Consequently, we aimed to compare metabolic cost calculated with the different models to metabolic cost measured with indirect calorimetry on walking trials with different speeds and slopes. These were used as test cases for intervention studies, since it requires a similar change in dynamics, while there is some information in literature of the effect of these dynamics changes to energy expenditure. It is known that in downhill walking, knee extensor activity increases [27, 28] while metabolic cost decreases [23], that in uphill walking metabolic cost increases [23], and that between 2 and 5 km/h, metabolic cost is independent of speed [29]. Therefore, a secondary goal is to see if the metabolic cost calculated with metabolic energy expenditure models has a similar effect with a change in slope or speed.

Methods

Subjects and experiment

Twelve healthy participants (6 female, 6 male, mean ± SD age 24 ± 5 years, weight 70 ± 12 kg, and height 173 ± 8 cm) provided informed consent prior to and performed the experiment. The experimental protocol was approved by the institutional review board of Cleveland State University (IRB-FY2017-286). First, the subjects stood on the treadmill for three minutes to determine their resting metabolic rate. They performed six walking trials of seven minutes in random order, three at 0.8 m/s and three at 1.3 m/s. For each speed, there were three different inclines: level walking, downhill walking with a negative incline of 8%, and uphill walking with a positive incline of 8%. Pulmonary gas exchange rates were measured with the COSMED K4b2 system (COSMED, Italy). An instrumented treadmill with two six degree of freedom force plates (R-Mill, Forcelink, Culemborg, the Netherlands) was used to measure the ground reaction forces. A motion capture system with 10 Osprey cameras and Cortex software (Motion Analysis, Santa Rosa, CA) was used to record 27 markers, given the markerset in S1 Figure and S1 Table. The raw and processed experimental data are published as a dataset in [30].

Metabolic energy models

Seven metabolic energy models were selected for this study: models BHAR04 [7], HOUD06 [10], UMBE03 [9], LICH05 [21], MINE97 [8], MARG68 [23], and KIMR15 [24]. Six models use muscle states (contractile element length, activation, stimulation) to determine the energy rate of the individual muscles. Model KIMR15 calculates the energy rate for each joint instead of each muscle, using the angular velocity and joint moment.

The calculated metabolic cost of walking, C_{calc}, is determined in J/kg/m as follows:

$$C_{calc} = \frac{1}{Tmv} \int_{t=0}^{T} \sum_{i=1}^{N_{mus}} \dot{E}_i \mathrm{d}t \tag{1}$$

where T denotes the motion duration, m the participant's mass, v the speed, N_{mus} the number of muscles, and $\dot{E}_i$ the energy rate of muscle i in W.

Models BHAR04, HOUD06, UMBE03, and LICH05 calculate the energy rate as a function of work rate, $\dot{w}$, and heat rates, due to activation, $\dot{h}_a$, maintenance of contraction, and $\dot{h}_m$, and muscle shortening and lengthening, $\dot{h}_{sl}$ [7, 9, 10, 21]:

$$\dot{E} = \dot{w} + \dot{h}_a + \dot{h}_m + \dot{h}_{sl} \tag{2}$$

The implementation of these models is detailed in S1 File.

Model MINE97 determines the energy rate for each muscle incorporating an empirical function of the ratio between the contractile element velocity, v_{CE} and the maximum contractile element velocity, $v_{CE(max)}$ [8]:

$$\dot{E} = aF_{max}v_{CE(max)}\phi \tag{3}$$

$$\text{where} \quad \phi = \frac{0.054 + 0.506\bar{v}_{CE} + 2.46\bar{v}_{CE}^2}{1 - 1.13\bar{v}_{CE} + 12.8\bar{v}_{CE}^2 - 1.64\bar{v}_{CE}^3} \tag{4}$$

where a is the muscle activation, F_{max} the maximum isometric force, and $\bar{v}_{CE}$ is the ratio of the contractile element velocity to the maximum contractile element velocity.

Model MARG68 is based on the observation that muscles are 25% efficient when

shortening, and 120% efficient when lengthening [23]:

$$\dot{E} = \begin{cases} \frac{\dot{w}}{0.25} & \text{if:} \quad v_{CE} < 0 \\ -\frac{\dot{w}}{1.2} & \text{if:} \quad v_{CE} \geq 0 \end{cases} \tag{5}$$

Model KIMR15 does not use muscle states, but calculates the metabolic rate on the joint level, using the joint moments and angular velocities. The metabolic rate is still the sum of the heat rate and the work [24]:

$$\dot{E}_i = \dot{h}_i + p_i \tag{6}$$

where the power, p, at joint i is the product of the joint moment M and angular velocity $\dot{\theta}$ [24]:

$$p_i = M_i \dot{\theta}_i \tag{7}$$

The heat rate is determined as follows [24]:

$$\dot{h}_i = \dot{h}_M \dot{q}_{i(max)} |M_i| + \dot{h}_{SL} |M_i \dot{q}_i| + \dot{q}_{cc} (M_i \dot{q}_i)_{max} \tag{8}$$

where $\dot{h}_M = 0.054$ is the heat rate for activation and maintenance, $\dot{h}_{SL} = 0.283$ is the shortening-lengthening heat rate for positive power, and $\dot{h}_{SL} = 1.423$ is the shortening-lengthening heat rate for negative power, and $\dot{q}_{cc}$ is the cocontraction heat rate. The subscript max indicates the maximum over the gait cycle [24].

Kinetic and Kinematic Data Processing

A two step approach was used calculate the joint angles, moments, and muscle states and inputs necessary to determine the metabolic cost of walking level, uphill and downhill using the metabolic energy models.

In the first step, the joint angles and moments were determined from marker and ground reaction force data. The data was filtered backwards and forwards with a second order Butterworth filter with a cut-off frequency of 6 Hz. Angles, angular velocities and accelerations, and segment accelerations were calculated from marker positions, velocities, and accelerations [31]. The data was split into gait cycles and

resampled to 100 data points per gait cycle.

The joint angles were determined using the orientation from the proximal to the distal marker on the body segment. For example, for the tibia these were the knee and ankle markers (RLEK/LLEK and RLM/LLM, see S1 Table and S1 Figure). The joint moments were determined from the marker data and the ground reaction forces using Winter's method [32]. The joint angles, moments, and ground reaction forces were averaged over all left and right gait cycles to find one average gait cycle.

In the second step, the muscle states (activation and contractile element length) and stimulations were determined using dynamic optimization method introduced in [33] such that the joint moments generated by the muscles matched the moments found using Winter's method. Fig 1 shows the eight Hill-type muscles that were modeled in each leg. These muscles were modeled as three element Hill-type muscles with quadratic springs for the parallel and series elastic element. The contractile element had activation dynamics, a force-length relationship, and a force-velocity relationship [15]. A full description of the muscle model and the muscle parameters are listed in S2 File.

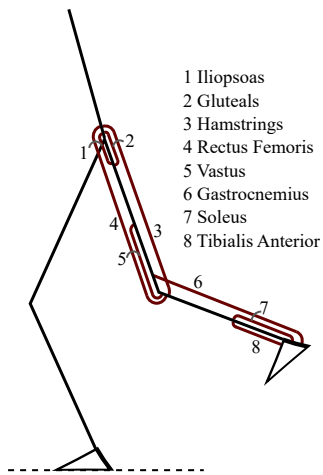

Fig 1. Schematic of the eight muscles that were used in this work.

The stimulations $u(t)$, activations $a(t)$, and contractile element lengths $l_{CE}(t)$ were

found by solving the following dynamic optimization problem:

$$\underset{l_{CE}(t),a(t),u(t)}{\text{minimize}} \quad \int_{t=0}^{T} \sum_{i=1}^{N_{mus}} a_i(t)^2 \mathrm{d}t \tag{9}$$

$$\begin{aligned} \text{Subject to:} & F_{SEE}(\theta(t)) - F_{PEE}(\theta(t)) \\ & - F_{CE}(a(t), l_{CE}(t), v_{CE}(t)) = 0 \qquad 0 \leq t \leq T \end{aligned} \tag{10}$$

$$\begin{aligned} & \dot{a} - (u(t) - a(t)) \\ & \left(\frac{u(t)}{T_{act}} + \frac{1-u(t)}{T_{deact}}\right) = 0 \qquad 0 \leq t \leq T \end{aligned} \tag{11}$$

$$DF_{SEE} - M_{winter} = 0 \qquad 0 \leq t \leq T \tag{12}$$

where F_{SEE}, F_{PEE} and F_{CE} denote the series elastic, parallel elastic and contractile element force, θ the joint angles, v_{CE} the contractile element velocity, the first derivative of the contractile element length. T_{act} is the activation time constant, T_{deact} is the deactivation time constant, D denotes a matrix of muscle moment arms, and M_{winter} the moments that were calculated previously. Periodic boundary conditions were used: $u(T) = u(0)$, $a(T) = a(0)$, and $l_{CE}(T) = l_{CE}(0)$.

This optimization problem was solved using direct collocation, with 100 nodes for the gait cycle and a Backward Euler formulation. IPOPT 3.11.0 was used to solve the optimization problem [34]. Finally, the muscle state trajectories and stimulations, or the joint angular velocities and moments were inserted in the seven metabolic energy models to find the calculated metabolic cost.

Pulmonary Data Processing

The measured metabolic cost was derived from the pulmonary gas exchange data using indirect calorimetry. The first 30 seconds of the resting trial, and the first three minutes of each walking trial were disregarded. The rate of oxygen consumption, $\dot{V}O_2$ in mL/min/kg, and respiratory quotient, R were averaged over time. The metabolic rate in W/kg was determined as follows for the resting and walking trials [35]:

$$W = \frac{4.184}{60}(3.941 + 1.106R)\dot{V}O_2 \tag{13}$$

The resting trial was subtracted from each walking trial. The metabolic rate was

divided by walking speed to find the measured metabolic cost in J/kg/m:

$$C_{meas} = \frac{W}{v} \tag{14}$$

Analysis

First, the implementation of the metabolic energy models was verified and compared to Miller [26]. To do so, the metabolic rate, $\dot{E}$, was determined for the soleus for three speeds (shortening at 1 l_{ce}/s, isometric and lengthening at 1 l_{ce}/s), and five activation levels (0.05, 0.25, 0.5, 0.75 and 1). The stimulation was assumed to be the same as the activation. The stimulation time, used in models BHAR04 and LICH05, was set to 1.

After the verification of the metabolic energy models, the metabolic cost was calculated for every subject and trial (Eq. 1) and compared to the measured metabolic cost (Eq. 2). Additionally, the calculated metabolic cost was determined for all joints individually. The metabolic cost of biarticular muscles was split between the joints on which they act using the ratios of the moment arms. The difference between the calculated and measured metabolic cost, averaged over all subjects, is also presented.

Finally, we investigated the ability of the metabolic energy models to predict a change in energy following a change in dynamics - due to altered walking speed and/or incline. Specifically, a repeated measures correlation [36] was used to determine how well the calculated metabolic cost correlated with the measured metabolic cost for every trial. A repeated measures analysis can account for the fact that more than one data point (i.e. different speeds and slopes) is available for each subject, which creates a dependency between the data points. This analysis accounts for multiple data points for each subject by assuming a model with the same slope for each subject, but a different intercept.

Results

Verification of Metabolic Energy Models

Fig 2 shows the metabolic power of the soleus muscle for several activation levels and a shortening and lengthening velocity of 1 $l_{CE(OPT)}$/s, where $l_{CE(OPT)}$ is the optimal

contractile element length, and an isometric condition. The metabolic rate for shortening is more than twice as high for model MARG68 than for all other models. In the isometric condition model MINE97 has the largest metabolic rate, while model MARG68 has zero metabolic rate, since no work is done at zero speed. The metabolic rate is most different between the models during lengthening, where models MARG68 and MINE97 had a positive metabolic rate, and the other models had a negative rate.

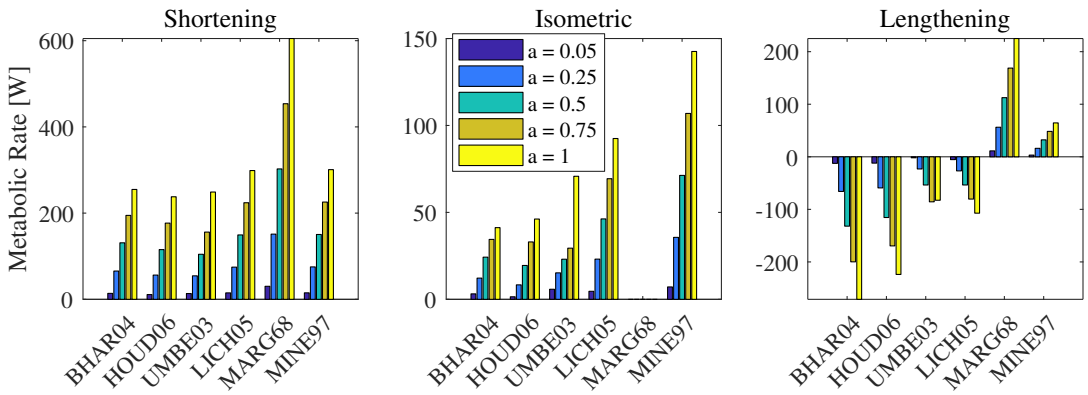

Fig 2. Metabolic rate of soleus, calculated with the metabolic energy models for different conditions. Metabolic rate as calculated by the metabolic energy expenditure models that are based on individual muscles of the soleus muscle at four activation levels, for an isometric condition, and a shortening and lengthening velocity of one optimal fiber length per second.

Joint Kinetics and Kinematics

Fig 3 shows the measured ground reaction forces, and the calculated joint angles, joint moments, and muscle forces for all trials at 1.3 m/s. In the uphill trials, the hip flexion angle, ankle dorsiflexion angle during stance, the hip flexion moment, and the ankle plantarflexion moment are larger, and more force is exerted by the gluteals, the hamstrings, and the gastrocnemius. In the downhill trials, the first vertical ground reaction force peak and the knee extension moment are larger, while the vastus, rectus femoris and tibialis anterior exert a larger force.

Fig 4 shows the measured ground reaction forces, and the calculated joint angles, joint moments, and muscle forces for all trials at 0.8 m/s. The pattern of the downhill, level, and uphill trials in the joint angles, moments, and ground reaction forces were very similar between the normal and the slow speed. The muscle forces also showed similar trends, but they were lower for the slow speed. One difference to normal speed is

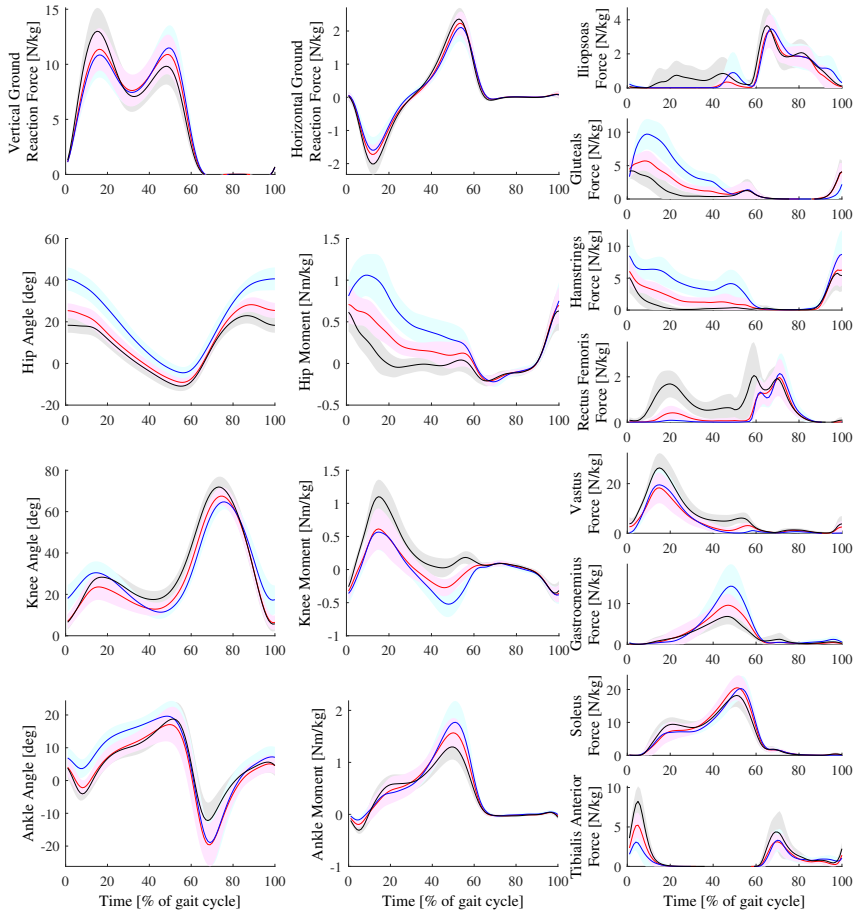

Fig 3. Kinetics and kinematics at the normal speed. Average ground reaction forces, joint angles, joint moments, and muscle forces for all trials at the normal speed (1.3 m/s). The shaded area denotes one standard deviation. The graphs use Winter's sign convention, where flexion angles and extension moments are positive for hip and knee. Dorsiflexion angle and plantarflexion moment are positive for the ankle.

the smaller peak in the soleus in the downhill trial.

Comparison of Calculated and Measured Metabolic Cost

Fig 5 shows the calculated metabolic cost for each model, separated for the hip, knee and ankle joints. Biarticular muscles were added by ratio of the moment arm, similar to [26]. The mean calculated metabolic cost was lowest for model HOUD06 and highest for model MARG68, ranging from 0.29 J/kg/m to 3.3 J/kg/m for the downhill trials, from 1.0 J/kg/m to 4.0 J/kg/m for the level trials and from 2.0 J/kg/m to 5.9 J/kg/m

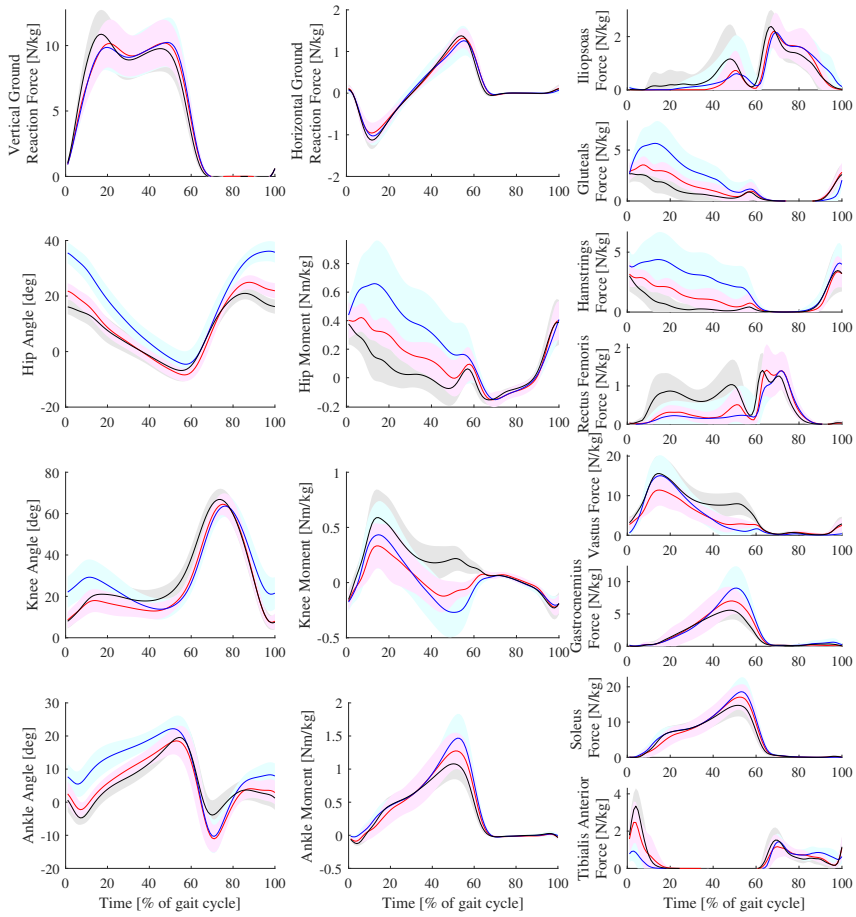

Fig 4. Kinetics and kinematics for the slow speed. Average ground reaction forces, joint angles, joint moments, and muscle forces for all trials at the slow speed (0.8 m/s). The shaded area denotes on standard deviation. The graphs use Winter's sign convention, where flexion angles and extension moments are positive for hip and knee. Dorsiflexion angle and plantarflexion moment are positive for the ankle.

for the uphill trials. The mean measured metabolic cost ranged from 2.0 J/kg/m for the downhill trial at 1.3 m/s to 5.9 J/kg/m for the uphill trial at 1.3 m/s (see bottom right graph). One measurement was missing for the downhill trial at 1.3 m/s due to a malfunction of the K4b2 system.

Comparing the different inclines, the calculated metabolic cost increased with incline for all models. The energy expenditure at the hip increased most from downhill to level to uphill walking. The metabolic cost calculated with model BHAR04 and model HOUD06 also increased at the knee and ankle joint with an increasing slope.

The effect of speed differed among the models. With model BHAR04, model HOUD06, model UMBE03, model LICH05, and model MINE97, the metabolic cost shifts from the knee to the ankle when the speed increases. For model UMBE03, model LICH05, and model MINE97, the summed metabolic cost of the knee and ankle is the same for both speeds. With model MARG68, there is an increase in metabolic cost at the ankle with speed, while for model KIMR15 there is an increase in the hip and ankle.

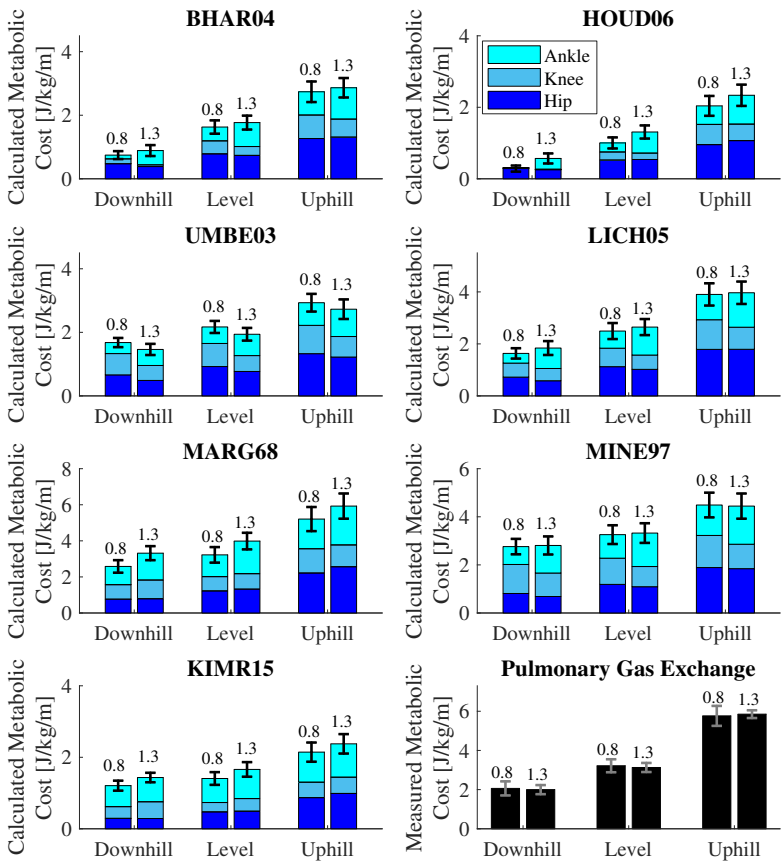

Fig 5. Calculated and measured metabolic cost for all trials and models. Calculated metabolic cost for all speeds and inclines, for each model, separately for the joints. The number above the bar indicates the speed of the trial. Biarticular muscles were added by ratio of the moment arm, similar to [26]

Fig 6 shows the difference between the measured metabolic cost and the calculated metabolic cost. Model MARG68 predicted three trials reasonably (the 95% confidence interval crosses zero), the uphill trials and the level trial at 0.8 m/s, and overestimated the other trials with less than 1 J/kg/m. Model MINE97 predicted the level trials

reasonably well, overestimated the downhill trials with about 0.7 J/kg/m, and underestimated the uphill trials with about 1.5 J/kg/m, while model LICH05 predicted the downhill trial at 1.3 m/s reasonably well, and model UMBE03 the downhill trial at 0.8 m/s. Model LICH05 underestimated the level trials with about 0.5 J/kg/m and the uphill trials with about 2 J/kg/m, while model UMBE03 underestimated with about 1 J/kg/m and 3 J/kg/m and model KIMR15 with about 2 J/kg/m and 3.5 J/kg/m, respectively for the level and uphill trials. Model KIMR15 also underestimated the downhill trials with 0.6 J/kg/m at 1.3 m/s and 0.9 J/kg/m at 0.8 m/s. Model BHAR04 underestimated the metabolic cost of the level and downhill trials with about 1 J/kg/m, and the uphill trials with about 3 J/kg/m. Model HOUD06 underestimated the level and downhill trials with about 2 J/kg/m, and the uphill trials with about 4 J/kg/m.

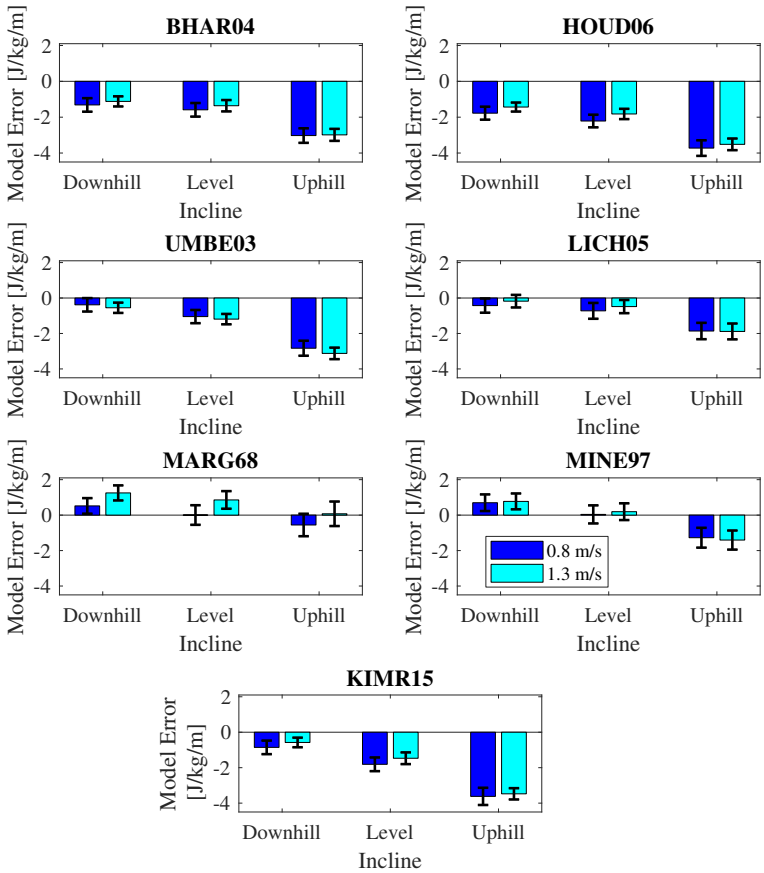

Fig 6. Average difference between measured and predicted metabolic cost with 95% confidence interval for all models and all trials.

Table 1. Results of repeated measures correlation. Repeated measures correlation coefficient r_{rm} [36] with 95% confidence interval (CI) and slope of the repeated measures model.

Model	r_{rm}	(95 % CI)	Slope
BHAR04	0.95	(0.92 - 0.97)	1.86
HOUD06	0.93	(0.88 - 0.96)	2.00
UMBE03	0.93	(0.89 - 0.96)	2.76
LICH05	0.95	(0.92 - 0.97)	1.65
MARG68	0.90	(0.83 - 0.94)	1.18
MINE97	0.94	(0.90 - 0.96)	2.05
KIMR15	0.90	(0.84 - 0.94)	3.32

Fig 7 shows the linear regression model that was fitted during the correlation analysis for each metabolic energy model. Table 1 shows the correlation coefficients of all models. All models correlate with a coefficient of at least 0.9. The highest correlation coefficient was 0.95 for model BHAR04 and model LICH05. The lowest correlation coefficient was 0.90 for model KIMR15 and model MARG68. The slope of the regression model for model MARG68 (1.18) was closest to unity, while the slope for model KIMR15 (3.32) was furthest away from unity.

Discussion

The goal of this paper was to compare metabolic cost calculated with seven metabolic models to metabolic cost measured with indirect calorimetry on walking trials with different speeds and slopes. Model BHAR04 and model LICH05 correlated best with the experimental data, while all models correlated with a coefficient of at least 0.9 (see table 1). The regression model of model MARG68 had a slope closest to unity, which indicates that this model calculates absolute differences between two trials most accurately. All models had a slope larger than one, meaning that the trials with higher metabolic demands were underestimated to a larger extent than those with a smaller metabolic demand, which is also visible in Fig 6. All models predicted a lower metabolic cost in the downhill trials than in the level trials, despite a larger force in the knee extensors (rectus femoris throughout stance and vasti during late stance), similar to observed in previous studies [23, 27, 28]. Model UMBE03 predicted a slightly lower metabolic cost for the larger speed, while model MINE97 predicted a similar cost between speeds, which is similar to the measured metabolic cost and [29], and the other

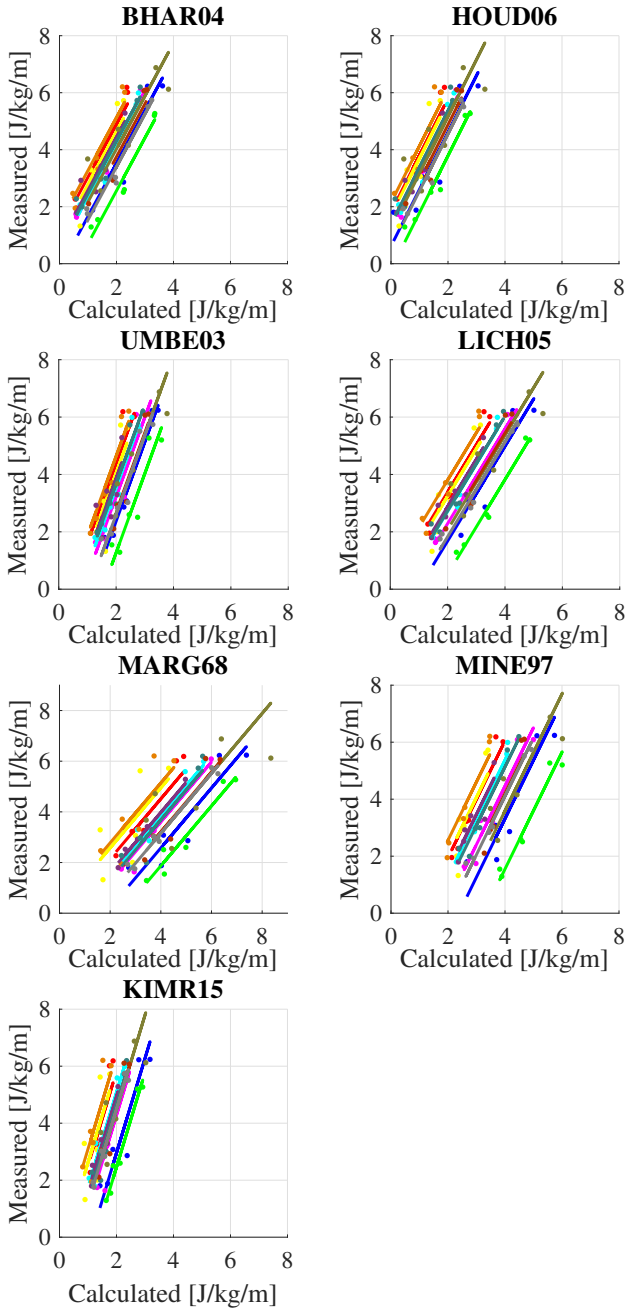

Fig 7. Correlation graphs for all models. Correlation graphs between calculated and measured metabolic costs for each model. The lines show the regression model that was fitted by the repeated measured correlation.

models predicted a slightly higher metabolic cost for the larger speed. The high correlation confirms Hicks et al. [37], who mention that a sagittal plane model should be sufficiently accurate for walking, since this motion is almost entirely in the sagittal plane. Correlation coefficients were also high for all subjects individually, except for one (purple line in Fig 7). This subject had an outlier of the uphill trial at slow speed.

The calculated metabolic cost is underestimated by all models, which is seen in Fig 6 for which three causes were identified. First, the underestimation could be due the approach used to find the muscle activations, where muscular effort was minimized, and any muscular co-contraction was disregarded. Secondly, the muscle mass was not adjusted with the subject's mass, while most models normalize the energy rate per muscle to the mass. Finally, the calculated metabolic cost could be lower since negative work was subtracted in this work. However, the high correlation indicates that the mechanical analysis still yielded a correct prediction of increases or decreases in metabolic cost.

The calculated metabolic cost in this study is also lower than calculated by Bhargava et al. [7] at 1.36 m/s (1.7 J/kg/m vs. 4.3 J/kg/m) and Umberger et al. [9] at 1.2 m/s: (1.9 J/kg/m versus 3.7 J/kg/m). Both studies also used some form of energy minimization objective. However, they do not report kinetics or kinematics and include a resting metabolic rate [7, 9]. Bhargava et al. also use a three dimensional model [7], while this work used a sagittal plane model with eight muscles and no resting metabolic rate. When accounting for a resting metabolic rate of 1.2 W/kg (see [9]), the metabolic cost was still higher than calculated in this work. A possible reason could be the low muscle mass in this model. The muscle mass was determined from the maximum isometric force, the total of which was a factor three lower than in a three dimensional model [38]. Model UMBE03 underestimated the increase in metabolic cost from level to uphill, and the decrease in metabolic cost from level to downhill. Dembia et al. [13] found a similar result using this model to predict the increase in metabolic cost from unloaded walking to loaded walking with 38 kg on the torso.

The handling of muscular energy expenditure during lengthening is still debated [26]. During lengthening, the energy rate can be negative, which is physically impossible. However, the negative work should be subtracted from the metabolic cost in models BHAR04, HOUD06, UMBE03, and LICH05 [7, 9, 10, 21]. We aimed to see if predictions

improved without this subtraction, which is physically more sensible. When negative work was not subtracted, the calculated metabolic cost increased. Model BHAR04 predicted the metabolic cost of the level trials correctly, model HOUD06 predicted the downhill trials correctly, model UMBE03 the level trial at 1.3 m/s and model LICH05 the uphill trial at 1.3 m/s. The correlation coefficient decreased by 0.01 for two models (BHAR04 and LICH05), 0.02 for model HOUD06, and 0.06 for model UMBE03. The lenghtening heat rate coefficient was updated in model UMBE03 according to [39], so it is interesting that the difference was largest for this model.

The kinematic and kinetic data are similar to previous studies of sloped walking [28, 40]. The trend of the muscle forces with the slope was similar to [41] for the gluteals, hamstrings, rectus femoris and gastrocnemius. This study used a model with 18 muscles in each leg, compared to eight in this work, which could explain the higher forces in the iliopsoas, hamstrings, vasti and soleus than in [41]. The force in the gluteals was lower, and the force in the rectus femoris, gastrocnemius and tibialis anterior was similar to [41]. Note that inaccuracies in the muscle force and activation could affect the results of all metabolic models.

The relative contribution of the different joints to the total metabolic cost in the level trial was smallest for the knee, between 14% and 26%, and similar between the hip and ankle, with the hip slightly smaller (between 29% and 41%) than the ankle (34% and 49%). Notably, model KIMR15 had the most unequal distribution between the hip and ankle, with 29% and 49%, while the other models had a difference in metabolic cost between these joints of less than 12%. This is similar to contributions of different joints in guinea fowl walking (24%, 37%, and 38% for the knee, hip and ankle, respectively), measured using their blood flow [42]. In [26], the relative contribution was reported for tracking simulations. For these simulation, the energy was distributed more evenly between all three joints, with the knee contributing between 27% and 34%, the hip between 23% and 39%, and the ankle between 29% and 50%, while the absolute metabolic cost varied greatly between models [26]. This suggest that some energy minimization is necessary to distribute energy between joints more accurately.

Similar trends existed between the metabolic energy models in the breakdown of the metabolic cost per joint, though differences exist in the breakdown for the specific trials (see Fig 5). Since no measurements were taken, it cannot be said which model is more

correct. However, the trends with speed and slope were very similar between models. The hip was mainly responsible for the change of energy expended with the slopes. When walking uphill, the energy expended in the hip increased, while it decreased when walking downhill. Between the speeds, the most obvious difference was a transfer of energy between joints, while the total metabolic cost remained similar. More energy was expended in the knee at 0.8 m/s, while more energy was expended in the ankle at 1.3 m/s.

Fig 2 showed that the models were correctly implemented. The results for models MINE97, BHAR04, HOUD06, LICH05, and UMBE03 were very similar to Fig 2 in [26]. Note that model UMBE03 in [26] does not allow negative work, so the result differs for lengthening.

It was observed in Fig 7 that the intercept of the repeated measures model was dependent on the weight of the subjects. A possible reason could be that the muscle mass was assumed the same between all subjects. When one is interested in calculating the absolute metabolic cost, and no measurements are available to determine the subject-specific intercept, the subject's mass could be used to improve the metabolic cost prediction using a linear model with two inputs: the calculated metabolic cost and the subject's mass. Such a model decreased the RMS error of the calculated metabolic cost between 33% and 68%, compared to the calculated metabolic cost. Further explanation of this model can be found in S3 File.

Commonly, muscle activations are found in gait analysis by static optimization [43] or computed muscle control (CMC) [44]. Static optimization only finds muscle activations, whereas model BHAR04 and model UMBE03 require activation and stimulation. All models, except model KIMR15, require the contractile element length and velocity. CMC requires a full-body model and markerset to solve for these variables. The approach in this work required only a lower-extremity model and six markers. A larger markerset was used to aid data processing in Cortex. Similar to static optimization [43], solutions were robust to changes in the objective function (Eq. 9). Optimizations with objectives of cubed activation, with and without muscle volume weighting, yielded similar muscle forces.

Other metabolic models were recently developed by Uchida et al. [22] and by Tsianos et al. [25]. The model by Uchida et al. was very similar to model UMBE03, but

it used a different method to determine the amount of fast twitch and slow twitch fibers. The results were very similar to model UMBE03, so they were not reported separately. The model by Tsianos et al. was not compatible with the musculoskeletal model that was used, since it is created for a different muscle model than a Hill-type muscle model, and was therefore not implemented.

Several equations have been developed to determine the energetic equivalent of pulmonary gas exchange measurements. Weir's equation is a standard, however has been shown to be inaccurate [45]. Therefore, the results were repeated with the equation presented by Peronnet [46]. The repeated measures correlation was the same using this equation as when Weir's equation was used. However, results were different in the absolute error (Fig 6), though a similar dependency on the subject's mass was present. Therefore, no further conclusions were drawn for the absolute predictions of the models.

Subjects were not asked to refrain from eating before the experiment. It is known that the peak influence of food on resting metabolic rate occurs after about 60 minutes for young adults [47], after which is slowly disappears [48]. Since the experimental set-up took at least 90 minutes, after which the measurements were taken relatively fast, and in a different order for each subject, it is expected that the effect is small. Using data from [47], and assuming the worst-case scenario that measurements were taken between 90 and 150 minutes after food intake, the effect would be around 0.2 W/kg, which is similar to the difference between Weir's and Peronnet's equation.

In summary, we have studied the ability of seven metabolic energy models to represent changes in energy cost of walking due to an altered environment. The full-body calculated metabolic cost of two models (BHAR04 and LICH05) correlated best with the metabolic cost of walking measured with indirect calorimetry. The subject's mass affected the calculated metabolic energy expenditure for all metabolic energy models. All models were able to predict the trend of increased metabolic cost from downhill to level to uphill walking, while the metabolic cost calculated with model MINE97 was most similar between the two speeds.

Supporting information

S1 File. Metabolic Energy Models. A description of the metabolic energy

models that were compared.

S2 File. Muscle Model. A description of the muscle model that was used to determine the stimulation, activation, and other muscle parameters.

S3 File. Repeated Measures Model with Weight-based Intercept. This supplementary file describes a repeated measures model with the intercept based on the subject's weight. This model can be used to determine the absolute metabolic energy expenditure using a metabolic energy model more accurately.

S1 Table. Marker description. Description of markers that were used in the experiment.

S1 Figure. Placement of markers on the body. Illustration of the placement of the markers that were used in the experiment on the body.

Acknowledgments

The authors would like to thank Dr. Ken Sparks and Chelsea Turowski for their help with gathering experimental data.

References

1. Ralston HJ. Energy-speed relation and optimal speed during level walking. Internationale Zeitschrift für Angewandte Physiologie Einschliesslich Arbeitsphysiologie. 1958;17(4):277–283.

2. Zarrugh M, Todd F, Ralston H. Optimization of energy expenditure during level walking. European Journal of Applied Physiology and Occupational Physiology. 1974;33(4):293–306.

3. Donelan J, Kram R, Kuo A. Mechanical and metabolic determinants of the preferred step width in human walking. Proceedings of the Royal Society of London B: Biological Sciences. 2001;268(1480):1985–1992.

4. Ortega JD, Farley CT. Minimizing center of mass vertical movement increases metabolic cost in walking. Journal of Applied Physiology. 2005;99(6):2099–2107.

5. Gordon K, Ferris D, Kuo A. Metabolic and mechanical energy costs of reducing vertical center of mass movement during gait. Archives of Physical Medicine and Rehabilitation. 2009;90(1):136–144.

6. Kenny GP, Notley SR, Gagnon D. Direct calorimetry: a brief historical review of its use in the study of human metabolism and thermoregulation. European journal of applied physiology. 2017;117(9):1765–1785.

7. Bhargava LJ, Pandy MG, Anderson FC. A phenomenological model for estimating metabolic energy consumption in muscle contraction. Journal of Biomechanics. 2004;37(1):81–88.

8. Minetti A, Alexander RM. A theory of metabolic costs for bipedal gaits. Journal of Theoretical Biology. 1997;186(4):467–476.

9. Umberger BR, Gerritsen KG, Martin PE. A model of human muscle energy expenditure. Computer methods in biomechanics and biomedical engineering. 2003;6(2):99–111.

10. Houdijk H, Bobbert M, De Haan A. Evaluation of a Hill based muscle model for the energy cost and efficiency of muscular contraction. Journal of Biomechanics. 2006;39(3):536–543.

11. Zajac FE, Neptune RR, Kautz SA. Biomechanics and muscle coordination of human walking: part II: lessons from dynamical simulations and clinical implications. Gait & posture. 2003;17(1):1–17.

12. Koelewijn AD, Van den Bogert AJ. Joint contact forces can be reduced by improving joint moment symmetry in below-knee amputee gait simulations. Gait & Posture. 2016;49:219–225.

13. Dembia CL, Silder A, Uchida TK, Hicks JL, Delp SL. Simulating ideal assistive devices to reduce the metabolic cost of walking with heavy loads. PloS one. 2017;12(7):e0180320.

14. Bregman D, Van der Krogt M, De Groot V, Harlaar J, Wisse M, Collins S. The effect of ankle foot orthosis stiffness on the energy cost of walking: a simulation study. Clinical Biomechanics. 2011;26(9):955–961.

15. Van den Bogert AJ, Hupperets M, Schlarb H, Krabbe B. Predictive musculoskeletal simulation using optimal control: effects of added limb mass on energy cost and kinematics of walking and running. Proceedings of the Institution of Mechanical Engineers, Part P: Journal of Sports Engineering and Technology. 2012; p. 1–11.

16. Dorn TW, Wang JM, Hicks JL, Delp SL. Predictive simulation generates human adaptations during loaded and inclined walking. PloS one. 2015;10(4):e0121407.

17. Miller R, Brandon S, Deluzio K. Predicting sagittal plane biomechanics that minimize the axial knee joint contact force during walking. Journal of Biomechanical Engineering. 2013;135(1):011007.

18. Huxley H. The double array of filaments in cross-striated muscle. The Journal of Biophysical and Biochemical Cytology. 1957;3(5):631–648.

19. Propp M. A model of muscle contraction based upon component studies. Lectures on Mathematics in the Life Sciences. 1986;16:61–119.

20. Winters J. Hill-based muscle models: a systems engineering perspective. In: Multiple Muscle Systems. Springer; 1990. p. 69–93.

21. Lichtwark GA, Wilson A. A modified Hill muscle model that predicts muscle power output and efficiency during sinusoidal length changes. Journal of Experimental Biology. 2005;208(15):2831–2843.

22. Uchida TK, Hicks JL, Dembia CL, Delp SL. Stretching your energetic budget: how tendon compliance affects the metabolic cost of running. PloS one. 2016;11(3):e0150378.

23. Margaria R. Positive and negative work performances and their efficiencies in human locomotion. European journal of applied physiology and occupational physiology. 1968;25(4):339–351.

24. Kim J, Roberts D. A joint-space numerical model of metabolic energy expenditure for human multibody dynamic system. International Journal for Numerical Methods in Biomedical Engineering. 2015;31(9).

25. Tsianos GA, Rustin C, Loeb GE. Mammalian muscle model for predicting force and energetics during physiological behaviors. IEEE Transactions on Neural Systems and Rehabilitation Engineering. 2012;20(2):117–133.

26. Miller RH. A comparison of muscle energy models for simulating human walking in three dimensions. Journal of biomechanics. 2014;47(6):1373–1381.

27. Lay AN, Hass CJ, Nichols TR, Gregor RJ. The effects of sloped surfaces on locomotion: an electromyographic analysis. Journal of biomechanics. 2007;40(6):1276–1285.

28. Pickle NT, Grabowski AM, Auyang AG, Silverman AK. The functional roles of muscles during sloped walking. Journal of biomechanics. 2016;49(14):3244–3251.

29. Margaria R. Biomechanics and Energetics of muscular exercise. Oxford University Press, USA; 1976.

30. Koelewijn AD, Heinrich D, van den Bogert AJ. Dataset for Metabolic Cost Calculations of Gait using Musculoskeletal Energy Models, a Comparison Study [Data set]; 2018.

31. Van den Bogert AJ, De Koning J. On optimal filtering for inverse dynamics analysis. In: Proceedings of the IXth biennial conference of the Canadian society for biomechanics. Simon Fraser University Vancouver; 1996. p. 214–215.

32. Winter DA. Biomechanics and motor control of human movement. John Wiley & Sons; 2009.

33. de Groote F, Kinney AL, Rao AV, Fregly BJ. Evaluation of direct collocation optimal control problem formulations for solving the muscle redundancy problem. Annals of biomedical engineering. 2016;44(10):2922–2936.

34. Wächter A, Biegler L. On the implementation of an interior-point filter line-search algorithm for large-scale nonlinear programming. Mathematical Programming. 2006;106(1):25–57.

35. Weir JdV. New methods for calculating metabolic rate with special reference to protein metabolism. The Journal of physiology. 1949;109(1-2):1–9.

36. Bakdash JZ, Marusich LR. Repeated measures correlation. Frontiers in Psychology. 2017;8.

37. Hicks JL, Uchida TK, Seth A, Rajagopal A, Delp SL. Is my model good enough? Best practices for verification and validation of musculoskeletal models and simulations of movement. Journal of biomechanical engineering. 2015;137(2):020905.

38. Hamner SR, Seth A, Delp SL. Muscle contributions to propulsion and support during running. Journal of biomechanics. 2010;43(14):2709–2716.

39. Umberger BR. Stance and swing phase costs in human walking. Journal of the Royal Society Interface. 2010;7(50):1329–1340.

40. Kimel-Naor S, Gottlieb A, Plotnik M. The effect of uphill and downhill walking on gait parameters: A self-paced treadmill study. Journal of Biomechanics. 2017;60:142–149.

41. Alexander N, Schwameder H. Effect of sloped walking on lower limb muscle forces. Gait & posture. 2016;47:62–67.

42. Ellerby DJ, Henry HT, Carr JA, Buchanan CI, Marsh RL. Blood flow in guinea fowl Numida meleagris as an indicator of energy expenditure by individual muscles during walking and running. The Journal of physiology. 2005;564(2):631–648.

43. Crowninshield RD, Brand RA. A physiologically based criterion of muscle force prediction in locomotion. Journal of biomechanics. 1981;14(11):793–801.

44. Delp S, Anderson F, Arnold A, Loan P, Habib A, John C, et al. OpenSim: open-source software to create and analyze dynamic simulations of movement. IEEE Transactions on Biomedical Engineering. 2007;54(11):1940–1950.

45. Kipp S, Byrnes WC, Kram R. Calculating metabolic energy expenditure across a wide range of exercise intensities: the equation matters. Applied Physiology, Nutrition, and Metabolism. 2018;43(6):639–642.

46. Peronnet F, Massicotte D, et al. Table of nonprotein respiratory quotient: an update. Can J Sport Sci. 1991;16(1):23–29.

47. Visser M, Deurenberg P, van Staveren WA, Hautvast JG. Resting metabolic rate and diet-induced thermogenesis in young and elderly subjects: relationship with body composition, fat distribution, and physical activity level. The American journal of clinical nutrition. 1995;61(4):772–778.

48. Compher C, Frankenfield D, Keim N, Roth-Yousey L, Group EAW, et al. Best practice methods to apply to measurement of resting metabolic rate in adults: a systematic review. Journal of the American Dietetic Association. 2006;106(6):881–903.